7836 J. Med. Chem. 2010, 53, 7836–7842
DOI: 10.1021/jm1009814

Journal of Medicinal Chemistry Article

Rational Design, Synthesis, and Evaluation of New Selective Inhibitors of Microbial Class II (Zinc Dependent) Fructose Bis-phosphate Aldolases

Racha Daher,[†,∥] Mathieu Coinçon,[§,∥] Matthieu Fonvielle,[†] Petra M. Gest,[‡] Marcelo E. Guerin,[‡,⊥] Mary Jackson,[‡] Jurgen Sygusch,*[,§] and Michel Therisod*[,†]

[†]*ECBB, ICMMO, Univ Paris-Sud, UMR 8182, F-91405 Orsay, France,* [‡]*Department of Microbiology, Immunology and Pathology, Mycobacteria Research Laboratories, Colorado State University, Fort Collins, Colorado 80523-1682, United States, and* [§]*Biochimie, Université de Montréal, CP 6128, Stn Centre-Ville Montréal, PQ H3C 3J7, Canada.* [∥]*These authors contributed equally to this work.* [⊥]*Present addresses: Unidad de Biofisica, Centro Mixto Consejo Superior de Investigaciones Cientificas − Universidad del País Vasco/Euskal Herriko Unibertsitatea (CSIC-UPV/EHU), Barrio Sarriena s/n, Leioa, Bizkaia, 48940, Spain, Departamento de Bioquímica, Universidad del País Vasco, Spain, and IKERBASQUE, Basque Foundation for Science, 48011, Bilbao, Spain.*

Received July 30, 2010

We report the synthesis and biochemical evaluation of several selective inhibitors of class II (zinc dependent) fructose bis-phosphate aldolases (Fba). The products were designed as transition-state analogues of the catalyzed reaction, structurally related to the substrate fructose bis-phosphate (or sedoheptulose bis-phosphate) and based on an N-substituted hydroxamic acid, as a chelator of the zinc ion present in active site. The compounds synthesized were tested on class II Fbas from various pathogenic microorganisms and, by comparison, on a mammalian class I Fba. The best inhibitor shows K_i against class II Fbas from various pathogens in the nM range, with very high selectivity (up to 10^5). Structural analyses of inhibitors in complex with aldolases rationalize and corroborate the enzymatic kinetics results. These inhibitors represent lead compounds for the preparation of new synthetic antibiotics, notably for tuberculosis prophylaxis.

Introduction

The resistance of pathogenic microorganisms to current antibiotics is a public health problem of major concern.[1] Factors contributing to this phenomenon are the emergence of resistant bacteria due to massive usage of antibiotics in human and veterinary medicine and the diffusion of the resistant bacteria in various ecosystems. The main consequences are: (1) an increase of nosocomial diseases contracted in hospitals: 5% of all hospitalized patients, at an annual cost exceeding 2 billion dollars per year resulting from infection by opportunistic pathogens such as *Pseudomonas aeruginosa*, *Candida albicans*, *Clostridium difficile*.[2] (2) A re-emergence of historic diseases such as tuberculosis (caused by *Mycobacterium tuberculosis*) and plague (infection by *Yersinia pestis*).[3] (3) A new threat of bioterrorism[4] that could make use of infectious agents such as *Bacillus anthracis* (anthrax), *Clostridium botulicum* (producing the botulic toxin), *Francisella tularensis* (agent of tularemia), *Coxiella burnetii* (Q fever), and *Richetsia prowasek* (typhus). Efficacious treatment of emerging antibiotic-resistant bacterial diseases thus requires alternatives to current antibiotic therapy. There is therefore a need to identify new microbial targets.

Because of their occurrence in many pathogenic microbes (bacteria, yeasts, parasites) and their absence in animals, class II fructose bis-phosphate aldolases (Fbas[a]) could be such promising new targets.

Aldolases (EC 4.1.2.13) are essential enzymes used in glycolysis, where they catalyze cleavage of fructose 1,6-bisphosphate (FBP) to yield dihydroxyacetone phosphate (DHAP) and glyceraldehyde-3-phosphate (G3P), and in gluconeogenesis and the Calvin cycle, where they catalyze the opposite reaction of triose-P condensation. These enzymes occur in two distinct classes. Class I Fbas, which are present in higher organisms (plants and animals) and some prokaryotes, form a Schiff-base intermediate between the keto substrate (FBP or DHAP) and a lysine residue of the active site. Class II Fbas in contrast, require a divalent metal ion (usually zinc or cobalt ion) to polarize the keto carbonyl group of the substrate (FBP or DHAP) and to stabilize the enediolate intermediate formed during catalysis (Figure 1). They are found exclusively in lower organisms such as yeasts, microalgae, protozoa, and bacteria, which include most pathogenic microorganisms mentioned above.

Of the Fba inhibitors that have been prepared, the very large majority display poor selectivity for class II versus class I Fbas and act as substrate analogues.[5] One notable exception is phospho-glycolohydroxamic acid (PGH),[6] considered to be either an analogue of the substrate DHAP or that of a high energy reaction intermediate (Figure 2). This compound has, however, only a hundred-fold selectivity for class II Fbas and has severe drawbacks that limit its potential use in vivo: (1) it is spontaneously hydrolyzed, releasing (toxic) hydroxylamine; (2) it is a powerful inhibitor of several other enzymes present both in mammals and microorganisms.

Other DHAP analogues have been reported with better selectivities (300−1000) but with lower potency.[7]

*To whom correspondence should be addressed. For J.S.: phone, 1 514 343 2389; fax, 1 514 343 6463; E-mail, jurgen.sygusch@umontreal.ca. For M.T.: phone, 33 1 69 15 63 11; fax, 33 1 69 15 72 81; E-mail, michel.therisod@u-psud.fr.

[a] Abbreviations: Fba, fructose bis-phosphate aldolase; FBP, fructose bis-phosphate; DHAP, dihydroxyacetone phosphate; G3P, glyceraldehyde-3-phosphate; PGH, phosphoglycolohydroxamic acid; SBP, sedoheptulose bis-phosphate; TS, transition state.

 Published on Web 10/07/2010

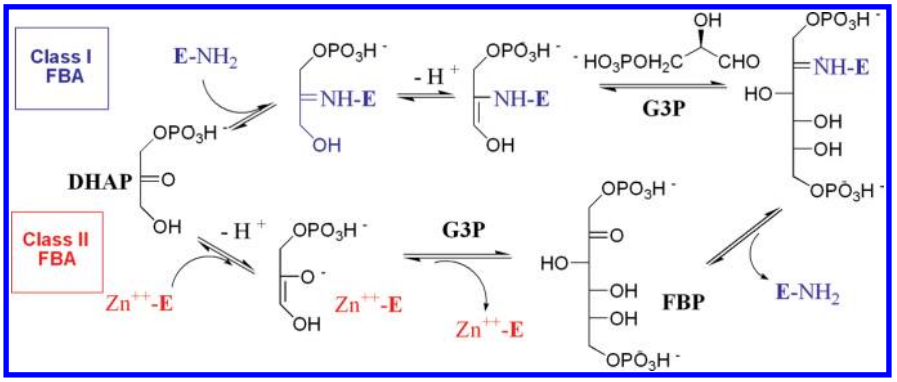

Figure 1. Mechanisms of class I (e.g., human) and class II (e.g., bacterial) Fbas.

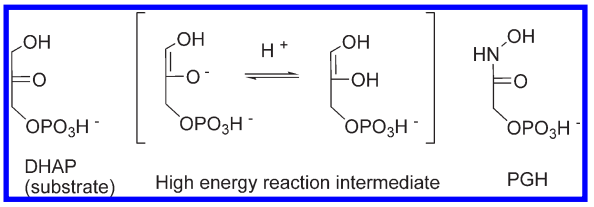

Figure 2. Structures of phosphoglycolo hydroxamic acid (PGH), DHAP (Fba substrate), and the high energy intermediate formed by deprotonation of DHAP.

We thus explored the use of compounds that are transition-state (TS) or high-energy intermediate analogues, whose structures are related to the substrate FBP, to improve inhibitory performances and selectivity.

Results and Discussion

Design of Inhibitors. We previously reported on the preparation and evaluation of *N*-(3-hydroxypropyl)-phosphoglycolohydroxamic acid bis-phosphate (**1′**) (Figure 3), a compound designed as an analogue of the natural substrate, FBP. **1′** gave encouraging results both in term of inhibitory power (K_i < 20 nM) and selectivity for the class II Fbas (> 20000).[8] This competitive inhibitor was shown by crystallographic analysis to bind within the active site of *Helicobacter pylori* Fba, a representative class II aldolase.

On this basis, we decided to prepare *N*-(4-hydroxybutyl)-glycolohydroxamic acid bis-phosphate (**1**), shown in Figure 3, with the following rationale for the design of a true selective transition-state analogue inhibitor:

(1) A well positioned hydroxamic acid function, responsible for the chelation of the transition metal zinc ion present at the active site of class II Fbas. The electronic delocalization in this functional group is intended to mimic the electronic density in the transition-state of the retro-aldol cleavage of FBP

(2) Two phosphate groups separated by an additional methylene group compared to **1′** to mimic sedoheptulose-1,7-bisphosphate (SBP), which is also a substrate for class II aldolases. K_M values for these two substrates are different, and in algal and cyanobacterial class II Fba, sedoheptulose-1,7-bisphosphate exhibits significantly tighter binding compared to FBP.[9] In addition, an increased distance between the two phosphate groups compared to FBP would more likely mimic the distance found in the transition state of the reaction.

(3) Furthermore *N*-alkylated hydroxamic acids are considerably more resistant to hydrolysis than the primary hydroxamate found in PGH.

The proposed analogue differs from the natural substrate FBP (SBP) in that the C4, C5 (C6) hydroxyl groups are absent. Consequently, the analogue does not possess asymmetric centers, which considerably simplifies its synthesis.

The designed structure of the inhibitor **1** makes it a very polar compound rendering passive transport across the cytoplasmic membranes of pathogenic bacteria or yeasts problematic. We therefore chose to study the inhibitory properties of monophosphorylated derivatives of **1** or a lipophilic ester in place of the P7 phosphate. If sufficiently active in vitro, *N*-(4-hydroxybutyl)-phospho-glycolohydroxamic acid (**2**), its hexanoyl ester (**3**), and its lauroyl ester (**4**) (Figure 4) could then act as lead compounds for the further synthesis of nonpolar prodrugs.[10]

Syntheses. The four new compounds were synthesized according to Schemes 1 and 2.

Biochemical Evaluation. The four compounds were tested in vitro as inhibitors of class II Fbas from various pathogenic species, using an inhibition assay previously reported.[8] For comparison and determination of selectivity, the compounds were also tested against a representative of mammalian class I Fba, isozyme A from rabbit muscle.

We first determined whether the microbial Fbas under study were indeed class II enzymes by conducting the enzymatic test in presence of 10 mM EDTA. Under these conditions, the four enzymes chosen were inhibited at more than 80%. By comparison, the rabbit enzyme (class I) in the same conditions retained full activity.

The analysis of the inhibition kinetics of these enzymes in presence of compounds **1**−**4** are reported in Table 1.

All four compounds tested show inhibitory activity and selectivity toward class II aldolases. As expected, compound **1** is by far the best inhibitor, with IC_{50} values in the nanomolar range with Fbas from *M. tuberculosis* and *C. albicans* and selectivities of up to 10^5. A 10-fold lower result was obtained with the enzyme from *Y. pestis*. A still less potent inhibition was observed on *H. pylori* Fba, with K_i and selectivity of 70 and 935 nM, respectively. These variations were unexpected in view of the high similarity among the reported structures of class II Fbas.[8,11−13] Interestingly, compounds **2**−**4**, lacking one phosphate group, retain selectivity (up to 10^4) and good inhibitory power (largely submicromolar) on three out of the four tested enzymes. The presence of a fatty ester on **3** and **4** does not change significantly K_i values, indicating that the compounds can be accommodated in the active site of class II Fbas. Thus, compounds **2**−**4** can be leads for the further synthesis of lipophilic prodrugs, more likely to cross biological membranes.[10] The best inhibitions were obtained on the *C. albicans* Fba. Consequently, this enzyme, considered as representative of the class II Fbas, was chosen for the determination of the type of inhibition. On this

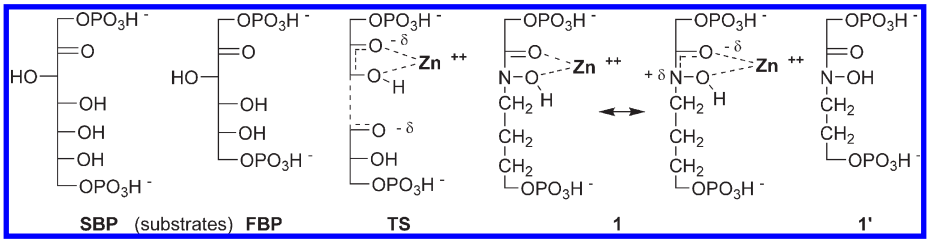

Figure 3. Fischer representations of sedoheptulose bis-phosphate, fructose bis-phosphate (SBP, FBP: substrates of Fba), of the transition state of the reaction catalyzed by a class II Fba (TS) and of the designed inhibitor **1** (and its mesomeric hybrid structure).

Scheme 1. Synthesis of Inhibitor **1**[a]

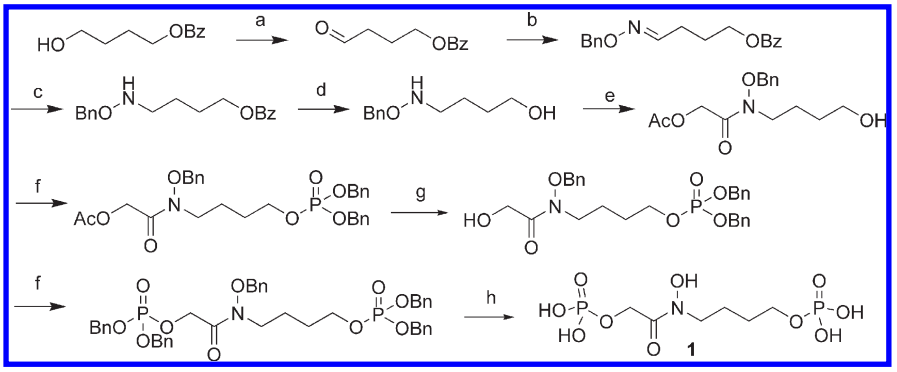

[a] (a) PCC; (b) $BnONH_2$; (c) $NaBH_3CN$; (d) MeONa; (e) $AcOCH_2COCl$ (f) $^{i}PrNP(OBn)_2$, then $^{t}BuOOH$; (g) NEt_3/MeOH; (h) $^{i}PrNP(OBn)_2$, then $^{t}BuOOH$; (i) H_2/Pd.

Scheme 2. Synthesis of Inhibitors **2**, **3**, **4**[a]

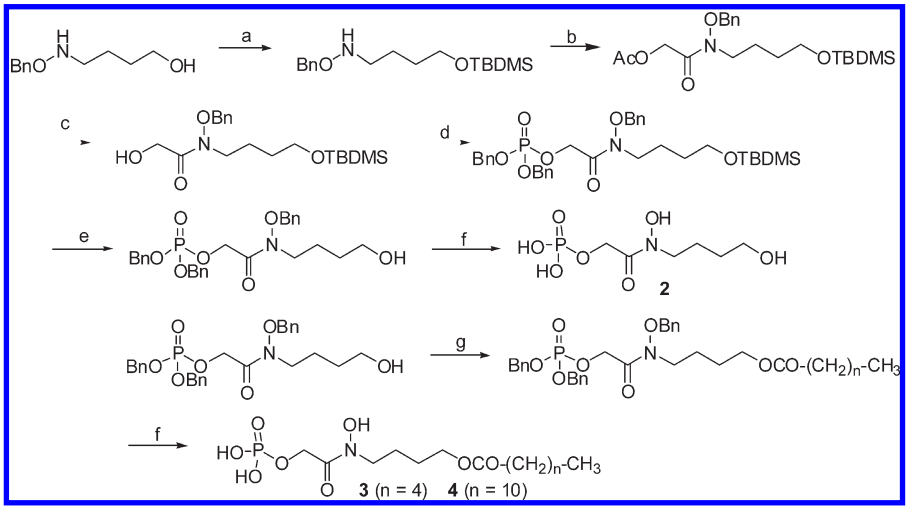

[a] (a) TBDMS-Cl; (b) $AcOCH_2COCl$; (c) NEt_3/MeOH; (d) $^{i}PrNP(OBn)_2$, then $^{t}BuOOH$; (e) Bu_4NF; (f) H_2/Pd-C; (g) hexanoyl or lauroyl chloride.

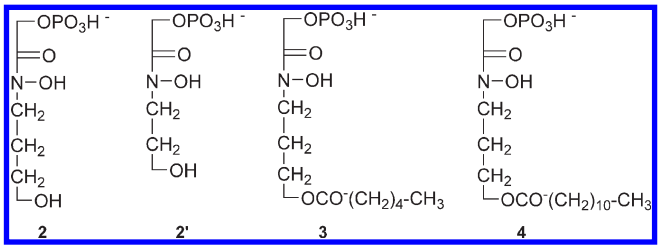

Figure 4. Monophosphorylated derivatives of **1**. (Compound **2′** is the monophosphorylated derivative of **1′**. Both compounds were previously described[8].)

enzyme, all four inhibitors **1**−**4** displayed competitive inhibition (see Supporting Information). The K_M/K_i value of up to 28000 obtained with **1** on *C. albicans* Fba is indicative of a transition-state analogue inhibitor rather than a simple substrate analogue.[14,15]

Crystallographic Results. The crystallographic structures of Fba from *H. pylori* bound with compounds **1** and **2** were solved to 1.85 Å and 1.8 Å resolution, respectively, in order to investigate the significant differences in affinity by compounds **1** and **2** among the class II aldolases shown in Table 1. Crystals of *H. pylori* Fba were grown by vapor diffusion as described previously.[8] *H. pylori* Fba structures in complex with **1** and **2** were solved by molecular replacement using *H. pylori* Fba complexed with **1′** (PDB 3C56)[8] as search model, and the structures corresponding to the best solution were refined and analyzed.

Table 1. In Vitro Biochemical Evaluation of Inhibitors

	K_M or K_i (μM)/(*selectivity*)[a]				
	class I Fba	class II Fbas			
compd	rabbit muscle	*H. pylori*	*C. albicans*	*M. tuberculosis*	*Y. pestis*
FBP (substrate)	15	17	85	21	55
1	57.5[b]	0.07[b](*935*)	0.003 (*1.1* × 10^5)	0.0016[b](*5* × 10^4)	0.018[b](*1.2* × 10^4)
2	400[b]	5.5[b](*82*)	0.30 (*7.5* × 10^3)	0.185[b](*3* × 10^3)	0.195[b](*7.25* × 10^3)
3	850	1[b](*950*)	0.28 (*1.7* × 10^4)	0.12[b](*9.7* × 10^3)	0.195[b](*1.6* × 10^4)
4	67	4[b] (*19*)	0.8 (*475*)	0.31[b](*305*)	0.234[b](*10^3*)
1′[8]	*264*[b]	0.013 (*2.3* × 10^4)	*0.2* (*7.5* × 10^3)[b]	*0.013* (*2.8* × 10^4)	
2′[8]	*2500*	*4.7* (*600*)	*0.416* (*3.4* × 10^4)	*0.17* (*2* × 10^4)	

[a] Expressed as $(K_M/K_{i\ class\ II})/(K_M/K_{i\ class\ I})$. [b] Calculated from IC_{50} values estimated with [S] = K_M.

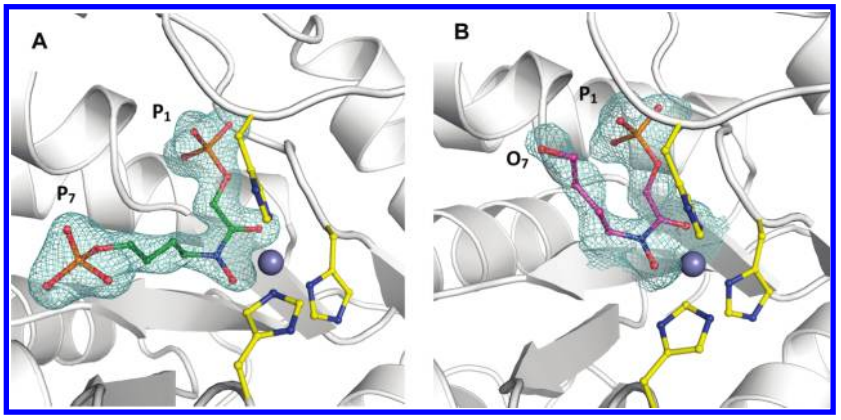

Figure 5. Difference electron density ($F_0 - F_C$) simulated annealed omit map showing fit to the electron density map by compounds **1** and **2** that are bound in the active site of *H. pylori* Fba. Binding by compound **1** is shown in (A), while that for compound **2** is shown in panel (B). P_1 and P_7 phosphates of **1** as well as O_7 atom of **2** are identified. Side chains for the histidine residues chelating the catalytic zinc ion are also depicted. Figure drawing and superposition were prepared using the program PyMOL.[16] The catalytic zinc ion is shown as a gray sphere in all figures. The electron densities shown were contoured at 3.5σ.

The compounds **1** and **2** bind in the active site of *H. pylori* Fba, consistent with their role as competitive inhibitors. The modes of active site binding for compounds **1** and **2** are shown in parts A and B of Figure 5, respectively.

The structural data obtained with **1** in *H. pylori* Fba reflects binding properties indicating that the interaction by the hydroxamate based inhibitor results in a loosely coordinated trigonal bipyramid geometry around the catalytic Zn^{2+} ion. Differences in the bound configurations of **1** and **2** are conditioned by the presence or absence of the P7-phosphate. In compound **1** bearing the P7-phosphate, the bound geometry is coincident with **1′** bound in *H. pylori* Fba previously reported[8] and shown in Figure 6. Although the binding sites for the P7-phosphate of **1** and the P6-phosphate of **1′** overlap substantially, there is a notable difference regarding oxyanion binding. In compound **1**, the P7-oxyanion loses an electrostatic interaction made by the P6-oxyanion of compound **1′** with Arg-259.

The longer alkyl carbon chain in **1** repositions the P7-oxyanion in the active site, abrogating the electrostatic interaction, and is replaced by a hydrogen bond between the P7-phosphate ester oxygen and W-7. The weaker strength of the hydrogen bond relative to the electrostatic interaction diminishes active site affinity by **1** compared to **1′** and is consistent with 5-fold greater K_i value for **1** than that reported for **1′**,[8] also shown in Table 1.

Compound **2** due to the absence of a P7-phosphate adopts an alternate configuration, with atoms C4, C5, C6, and O7 pointing out of the active site. Electron density delineating the configuration of compound **2** in each asymmetric unit cell was well-defined for four of the eight protomers and was

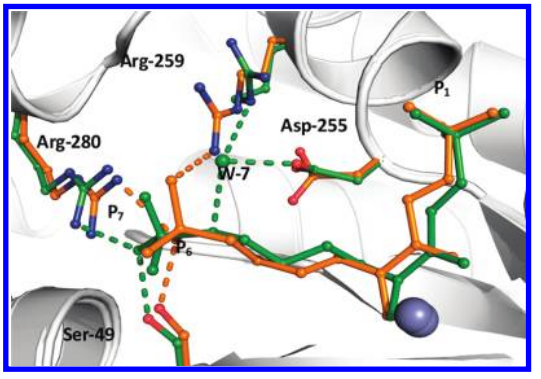

Figure 6. Differences in binding modes between compounds **1′** (orange) and **1** (green) in *H. pylori* Fba. The P6-phosphate in **1′** participates in electrostatic interactions with Arg-259 and Arg-280 and one hydrogen bond with Ser-49. In **1**, the P7-phosphate loses its charged interaction with Arg-259, replaced by a hydrogen bond with W-7.

characterized by O7 interacting solely with water molecules. A representative fit by compound **2** to the electron density in these asymmetric unit cells is shown in Figure 5B. In the remaining asymmetric unit cells, carbon atoms C4−C7 and O7 of compound **2** were fitted to progressively weaker electron density that corresponded to a slightly different traces for these atoms. In this secondary configuration, O7 interacted with its phosphate oxyanion. Superimposition of compound **2** from all asymmetric subunits indicated considerable configurational heterogeneity, notably for the positions of the terminal C7 and O7 atoms (rmsd for C7 and O7 were 0.82 and 1.01 Å, respectively). The absence of the P7-phosphate

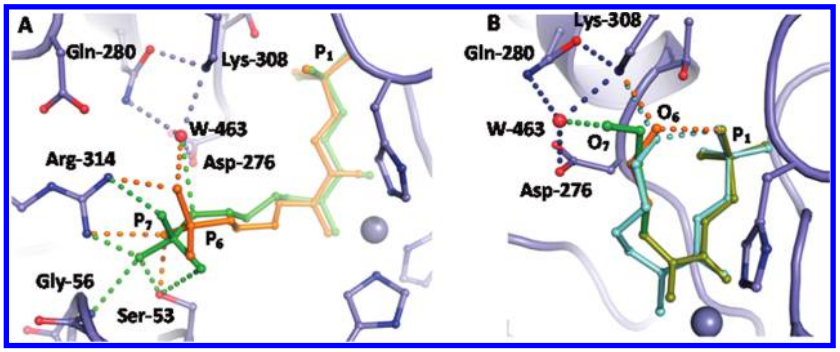

Figure 7. Modeling of compounds **1′**, **1**, **2**, and **2′** into active site of *M. tuberculosis* Fba active site. Interactions made by **1′**, **1**, **2**, and **2′** with active site residues other than with their alkyl fractions are identical among the two Fbas. (A) Interactions made by the P6-phosphate of **1′** (orange) and the P7-phosphate of **1** (green); (B)interactions made by the O6 atom in **2′** (monophosphorylated form of **1′** without the P6-phosphate) (orange) and O7 atom in **2** (green). (B) interactions also made by O7 in a representative secondary configuration (cyan) fitted for compound **2**. Water molecule W-463 positioned through hydrogen bonding with Asp-276, Gln-280, and Lys-308 is shown in orange. View was obtained by overlaying structures of *H. pylori* Fba bound by **1′** and *M. tuberculosis* Fba bound with FBP.

moiety in **2** decreases affinity by nearly 2 orders of magnitude shown from Table 1 and reflects a similar loss in binding affinity by compound **2′** (the monophosphorylated form of **1′** lacking the P6-phosphate) compared to **1′**, shown in Table 1. In the bound configuration, the hydroxamate moiety of **2** coordinates the Zn ion in a coplanar geometry, mimicking an enediolate transition-state that could partially compensate for the loss in binding affinity by **2** due to the absence of the P7-phosphate.

Superposition of native Fba with each bound Fba (rmsd < 0.5 Å, based on all Cα atoms) indicates the same localized conformational changes induced upon binding, reported previously,[8] allowing efficient interaction with the P_1 phosphate of each compound. Concomitantly with this conformational movement, the catalytic zinc ion displaces by 3.7 Å from its buried position in the native structure toward the active site surface, chelating C=O and N−O oxygens of **1** and **2** while maintaining its interaction with the chelating His residues of the active site. The identical conformational responses to compounds **1** and **2** binding (also previously observed with **1′**) indicate that the differential interaction by the alkyl fraction of these compounds with the active site modulates their binding affinity rather than differential conformational responses by *H. pylori* Fba to binding by compounds **1** and **2**.

M. tuberculosis aldolase in complex with FBP (PDB 3ELF)[17] was next used as a surrogate template to model interactions made by *M. tuberculosis* aldolase with compounds **1′**, **1**, and **2**. Modeling consisted of superimposing the structures of *H. pylori* aldolase in complex with compounds **1′**, **1**, and **2** onto the structure of *M. tuberculosis* aldolase in complex with FBP using the Align function in the program PyMOL (rmsd < 1 Å based on 175 superimposed Cα atoms). The superimposition coincided FBP phosphate oxyanions with those of the **1′** analogue and closely aligned the positions of the homologous backbone carbons of **1′** with those of FBP (Figure 1, Supporting Information). The match of FBP with the positions of **1′** corroborates use of the structure of *M. tuberculosis* aldolase in complex with FBP as a good surrogate template to probe the response of *M. tuberculosis* aldolase to active site ligand binding events.

The superimposition highlighted active site differences that rationalized trends in binding affinity between the two Fbas. A significant difference is the electrostatic interaction made in *H. pylori* Fba between the **1′** P6-oxyanion and an arginine, Arg-259, which does not have a homologue in *M. tuberculosis* Fba. Instead, in *M. tuberculosis* Fba, the P6-oxyanion electrostatic interaction is replaced by a hydrogen bond to a water molecule W-463 that maximizes its hydrogen bonding interaction with three additional active site residues, Lys-308, Asp-276, and Gln-280, shown in Figure 7A. The hydrogen bond interaction is complemented by an additional electrostatic interaction, albeit weaker between the P6-oxyanion and Arg-314 (3.1 Å). Identical K_i values for **1′** in both Fbas and also very similar K_M values, according to Table 1, suggests that these two interactions in *M. tuberculosis* Fba compensate for the loss of the strong electrostatic interaction made in *H. pylori* Fba.

The interaction of **1** with *M. tuberculosis* Fba, as shown in Figure 7A, results in formation of an additional H-bond between the P7-oxyanion and a backbone amide of Gly-56 that does not occur in *H. pylori* Fba. In *H. pylori* aldolase, the homologous residue, Ala-52, points its methyl group toward the P7-oxyanion, precluding additional hydrogen bonding and corroborating the greater affinity (estimated through the inhibitory activity) by **1** for *M. tuberculosis* Fba compared to **1′**, shown in Table 1. This difference in active site residues, Ala-52 in *H. pylori* Fba versus Gly-56 in *M. tuberculosis* Fba, rationalizes the inverse trend in binding affinity for **1** between these two class II Fbas.

Figure 7B shows the results of the modeling of **2** into the active site of *M. tuberculosis* aldolase (PDB 3ELF). In contrast to *H. pylori* Fba, where O7 in **2** does not interact with active site residues, superimposition of **2** onto *M. tuberculosis* Fba indicates additional stabilization of binding by compound **2**. Although direct superimposition of compound **2**, as shown in Figure 5B, introduces an apparent steric conflict between Lys-308 Cα and O7 atom of **2**, the steric clash can be relieved by slight displacement of the terminal alkyl chain in **2** (0.6 Å) that is comparable in magnitude to the rmsd value of the configurational heterogeneity observed for atoms C7 and O7. In this unencumbered configuration, O7 of **2** is able to hydrogen bond with water molecule Wat-463 that enhances its interaction with the active site in *M. tuberculosis* aldolase. In its secondary configuration, superposition enables compound **2** to interact with Lys-308 while maintaining its interaction with its own oxyanion. Compound **2′**, lacking the P6-phosphate in **1′**, can be modeled bound isostructurally with **2**, as shown in Figure 5B, and allowing its O6 atom to form a hydrogen bond with Lys-308 as well as with its own

oxyanion, shown in orange in Figure 7B. The additional hydrogen bond made by compounds, **2** and **2′** in *M. tuberculosis* Fba are consistent with their greater active site binding affinity in *M. tuberculosis* Fba compared to *H. pylori* Fba, shown in Table 1.

Multiple alignment of class II Fba (Table 2, Supporting Information) supports greater active site similarity between the Fba enzymes of *C. albicans*/*Y. pestis* and *M. tuberculosis* than with the *H. pylori* Fba. Active site residues that contact compounds **1′**, **1**, and **2** in *M. tuberculosis* Fba are conserved in *C. albicans* and *Y. pestis* Fba, including the residues homologous to Gly-56 and Gln-280. Indeed, compounds **1** and **2** exhibit tighter inhibitions of *C. albicans* and *Y. pestis* Fbas similar to *M. tuberculosis* Fba, as seen in Table 1, compared to *H. pylori* Fba. These two residues rationalize the differential response to active site binding by compounds **1′**, **1**, and **2** within class II Fbas. The modification of compound **2** by the addition of lipophilic esters does not significantly impact binding affinity for compounds **3** and **4** for all class II Fbas, shown in Table 1, and would indicate that lipophilic esters do not interact with active residues and likely point toward the bulk solution.

Compound **1** differs from aldolase substrate sedoheptulose-1,7-bisphosphate in the absence of hydroxyl moieties at C_4, C_5, and C_6 atoms. In class I aldolase, K_M values determined with sedoheptulose-1,7-bisphosphate are comparable with those determined for FBP.[9] We postulate that **1**, in lacking hydroxyl moieties at atom positions C4, C5, and C6, reduces its ability to participate in hydrogen bonding interactions with active site residues of class I aldolase and, together with the apparent coplanarity of hydroxamate moiety atoms in **1**, would further hinder optimal fit into class I aldolase active site and forms an additional basis for high selectivity of **1** for class II aldolases. Future design would exploit stereochemical differences introduced at C_4, C_5, and/or C_6 atoms with respect to FBP and sedoheptulose-1,7-bisphosphate substrates in order to enhance inhibitor potency.

Antibacterial Evaluation. Compounds **1**−**4** were assayed by standard procedures[18,19] for inhibition of growth of cultivated microorganisms: *M. tuberculosis*, *C. albicans*, *Y. pestis*. No inhibition was observed at concentrations up to 1 mM.

Conclusion

We have prepared and evaluated the most powerful and selective inhibitor of class II Fba reported so far. Nonphosphorylated derivatives of this compound, although less potent, may serve as lead candidates for the synthesis of prodrugs to be tested on cultivated pathogenic species. The detailed structural analysis, in full accordance with the kinetics data, indicates that the design of potent hydroxamate based inhibitors for class II Fbas is conditioned by the absence or presence of specific nonhomologous active site residues. These differences can be exploited in the design of more potent and selective inhibitors for therapeutic gain. No inhibition of growth of cultivated pathogens however was observed so far with compounds **1** − **4**, most probably as a consequence of the presence of phosphate groups. We propose to synthesize lipophilic prodrugs of the best inhibitors and/or products bearing phosphomimetic groups.

Methods

Enzymes. The four class II Fbas were purified recombinant enzymes, expressed in *E. coli*. class I Fba from rabbit muscle, was purchased from Sigma.

Enzymatic Test. Fructose bisphosphate and inhibitor, made up at the appropriate concentration in a glycyl-glycine buffer (0.1 M pH 7.4, 0.2 M in AcOK), NADH (0.12 mM), glycerophosphate dehydrogenase (11 U), triose-phosphate isomerase (3 U), and aldolase (4 mU), were placed in a cuvette to give a final volume of 1.2 mL. The decrease in absorbance of NADH at 340 nm was monitored on a spectrophotometer over 1−2 min.

Chemical Syntheses. The complete procedure is given in the Supporting Informations. The determinations of purity of the four synthesized compounds were performed with a Perkin-Elemer HPLC system using a Hypersil ODS C18 analytical column (250 mm × 4.6 mm) and a linear gradient solvent system: 0.1 M triethylammonium acetate buffer:CH_3CN in ratios from 95/5 to 40/60 for 20 min with flow rate 1 mL/min. Peaks were detected by UV absorption using a diode array detector. Retention times, min (purity): **1**, 4.5 min (95%); **2**, 6.8 (96%); **3**, 8.7 (96%); **4**, 10.2 (95%).

Selected analytical data for compounds **1**−**4**:

1 (**Disodium Salt**). ^{1}H NMR (250 MHz, D_2O): δ 4.5 (d, J = 6.5 Hz, 2H), 3.7 (q, J = 6.25 Hz, 2H), 3.5 (t, J = 6.25 Hz, 2H), 1.56−1.44 (m, 2H), 1.62−1.56 (m, 2H). ^{13}C NMR (62.5 MHz, BB, D_2O): δ 171.0, 170.86, 65.0, 64.92, 61.8, 47.88, 27.0, 26.89, 22.11. ^{31}P NMR (101.25 MHz, BB, D_2O): δ 1.85, 0.95.

HR-MS (ESI negative): m/z 322.0088 (calcd for $C_6H_{14}NO_{10}P_2$: 322.0093).

2 (**Monosodium Salt**). ^{1}H NMR (250 MHz, D_2O): δ 4.49 (d, J = 6.25 Hz, 2H), 3.52 (t, J = 6.5 Hz, 2H), 3.48 (t, J = 6.5 Hz, 2H), 1.52 (p, J = 6.5 Hz, 2H), 1.42 (t, J = 6.5 Hz, 2H). ^{13}C NMR (62.5 MHz, BB, D_2O): δ 171, 61.63, 61.18, 47.90, 28.29, 22.18. ^{31}P NMR (101.25 MHz, BB, D_2O): δ 2.47.

HR-MS (ESI negative): m/z 242.0429 (calcd for $C_7H_{13}NO_7P$: 242.0430).

3 (**Monosodium Salt**). ^{1}H NMR (250 MHz, D_2O): δ 4.5 (d, J = 5.7 Hz, 2H), 4.05 (t, J = 5.85 Hz, 2H), 3.55 (t, J = 5.8 Hz, 2H), 2.29 (t, J = 7.5 Hz, 2H), 1.66−1.4 (m, 6H), 1.30−1.10 (m, 4H), 0.77 (t, J = 6.9 Hz, 3H). ^{13}C NMR (62.5 MHz, BB, D_2O): δ 177.56, 64.82, 61.51, 47.81, 34.02, 30.54, 25.02, 24.13, 22.46, 21.64, 13.21. ^{31}P NMR (101.25 MHz, BB, D_2O): δ 3.72.

HR-MS (ESI negative): m/z 340.1163 (calcd for $C_{12}H_{23}NO_8P$: 340.1161).

4 (**Monosodium Salt**). ^{1}H NMR (250 MHz, D_2O): δ 4.51 (d, J = 4.0 Hz, 2H), 4.07−3.93 (m, 2H), 3.58 − 3.45 (m, 2H), 2.2 (t, J = 6 Hz, 2H), 1.66−1.42 (m, 6H), 1.29−1.05 (m, 16H), 0.75 (t, J = 6 Hz, 3H). ^{13}C NMR (62.5 MHz, BB, D_2O): δ 174.6, 64.37, 61.63, 34.11, 32.0, 29.85−29.3, 25.36, 24.86, 22.66, 22.53, 13.85. ^{31}P NMR (101.25 MHz, BB, D_2O): δ 3.78.

HR-MS (ESI negative): m/z 424.2113 (calcd for $C_{18}H_{35}NO_8P$: 424.2100).

Acknowledgment. We are very grateful to Dr. Jean-Michel Bruneau (NOVEXEL, Romainville, France) for the kind supply of recombinant Fba from *C. albicans*. J.S. was supported by funding from Natural Science and Engineering Research Council (Canada) and Canadian Institutes for Health Research. R.D. was supported by a scholarship from the Region Ile de France. M.J. is supported by the National Institute of Allergy and Infectious Diseases (NIAID), National Institutes of Health (NIH) grant AI078126 and the National Institute of Neurological Disorders and Stroke (NINDS), NIH grant NS066438.

Supporting Information Available: Detailed syntheses of compounds **1**−**4**. Determinations of IC_{50} and K_i. Structure solution of *H. pylori* Fba complexes with compounds **1** and **2**. Multiple alignment of class II FBP aldolases. This material is available free of charge via the Internet at http://pubs.acs.org.

References

(1) Soulsby, E. J. Resistance to antimicrobials in humans and animals. *Br. Med. J.* (*Clin. Res. Ed.*) **2005**, *331*, 1219–1220.

(2) Mc Fee, R. B. Nosocomial or hospital-acquired infections: an overview. *Disease-A-Month* **2009**, *55*, 422–438.

(3) (a) Maartens, G.; Wilkinson, R. J. Tuberculosis. *Lancet* **2007**, *370*, 2030–2043. (b) Prentice, M. B.; Rahalison, M. Plague. *Lancet* **2007**, *369*, 1196–1207.

(4) World, M. J. Bioterrorism. The need to be prepared. *Clin. Med.* **2004**, *4*, 161–164.

(5) Gefflaut, T.; Blonski, C.; Perie, J.; Willson, M. Class I aldolases: substrate specificity, mechanism, inhibitors and structural aspects. *Prog. Biophys. Mol. Biol.* **1995**, *63*, 301–340.

(6) Collins, K. D. An activated intermediate analogue. The use of phosphoglycolohydroxamate as a stable analogue of a transiently occurring dihydroxyacetone phosphate-derived enolate in enzymatic catalysis. *J. Biol. Chem.* **1974**, *249*, 136–142.

(7) Fonvielle, M.; Weber, P.; Dabkowska, K.; Therisod, M. New highly selective inhibitors of class II fructose-1,6-bisphosphate aldolases. *Bioorg. Med. Chem. Lett.* **2004**, *14*, 2923–2926.

(8) Fonvielle, M.; Coinçon, M.; Daher, R.; Desbenoit, N.; Kosieradzka, K; Barilone, N.; Gicquel, B.; Sygusch, J.; Jackson, M.; Therisod, M. Synthesis and biochemical evaluation of selective inhibitors of class II fructose bis-phosphate aldolases: towards new synthetic antibiotics. *Chem. Eur. J.* **2008**, *14*, 8521–8529.

(9) (a) Flechner, A.; Gross, W.; Martin, W. F.; Schannenberger, C. Chloroplast class I and class II aldolases are bifunctional for fructose-1,6-biphosphate and sedoheptulose-1,7-biphosphate cleavage in the Calvin cycle. *FEBS Lett.* **1999**, *447*, 200–202. (b) Nakahara, K.; Yamamoto, H.; Miyake, C.; Yokota, A. Purification and characterization of class I and class II fructose-1,6-bisphosphate aldolases from the cyanobacterium Synechocystis sp. PCC 6803. *Plant Cell. Physiol.* **2003**, *44*, 326–333. (c) Erales, J; Avilan, L; Lebreton, S; Gontero, B. Exploring CP12 binding proteins revealed aldolase as a new partner for the phosphoribulokinase/glyceraldehyde 3-phosphate dehydrogenase/CP12 complex purification and kinetic characterization of this enzyme from Chlamydomonas reinhardtii. *FEBS J.* **2008**, *275*, 1248–1259.

(10) Schultz, C. Prodrugs of biologically active phosphate esters. *Bioorg. Med. Chem.* **2003**, *11*, 885–898.

(11) Hall, D. R.; Leonard, G. A.; Reed, C. D.; Watt, C. L.; Berry, A.; Hunter, W. N. The crystal structure of *Escherichia coli* class II fructose-1,6-bisphosphate aldolase in complex with phosphoglycolohydroxamate reveals details of mechanism and specificity. *J. Mol. Biol.* **1999**, *287*, 383–394.

(12) Galkin, A.; Kulakova, L.; Melamud, E.; Li, L.; Wu, C.; Mariano, P.; Dunaway-Mariano, D.; Nash, T. E.; Herzberg, O. Characterization, kinetics, and crystal structures of fructose-1,6-bisphosphate aldolase from the human parasite, *Giardia lamblia*. *J. Biol. Chem.* **2007**, *282*, 4859–4867.

(13) Izard, T; Sygusch, J. Induced fit movements and metal cofactor selectivity of class II aldolases: structure of *Thermus aquaticus* fructose-1,6-bisphosphate aldolase. *J. Biol. Chem.* **2004**, *279*, 11825–11833.

(14) Kurz, J. L. Transition state characterization for catalyzed reactions. *J. Am. Chem. Soc.* **1963**, *85*, 987–991.

(15) Wolfenden, R. Transition state analogues for enzyme catalysis. *Nature* **1969**, *223*, 704–705.

(16) DeLano, W. L. *The PyMOL Molecular Graphics System*; DeLano Scientific LLC: San Carlos, CA2004.

(17) Pegan, S. D.; Rukseree, K.; Franzblau, S. G.; Mesecar, A. D. Structural basis for catalysis of a tetrameric class II fructose 1,6-bisphosphate aldolase from *Mycobacterium tuberculosis*. *J. Mol. Biol.* **2009**, *386*, 1038–1053.

(18) Bai, N. J.; Pai, M. R.; Murthy, P. S.; Venkitasubramanian, T. A. Effect of oxygen tension on the aldolases of *Mycobacterium tuberculosis*. *FEBS Lett.* **1974**, *45*, 68–70.

(19) Martin, A.; Camacho, M.; Portaels, F.; Palomino, J.-C. Rezazurin microtiter assay plate testing of *Mycobacterium tuberculosis* susceptibilities to second-line drugs: rapid, simple and inexpensive method. *Antimicrob. Agents Chemother.* **2003**, *47*, 3616–3619.